Noise model for serrated trailing edges compared to wind tunnel measurements

Fischer, Andreas; Bertagnolio, Franck; Shen, Wen Zhong; Madsen, Jesper

Published in:
Journal of Physics: Conference Series (Online)

Link to article, DOI:
10.1088/1742-6596/753/2/022053

Publication date:
2016

Document Version
Publisher's PDF, also known as Version of record

Noise model for serrated trailing edges compared to wind tunnel measurements

2016 J. Phys.: Conf. Ser. 753 022053

(http://iopscience.iop.org/1742-6596/753/2/022053)

Noise model for serrated trailing edges compared to wind tunnel measurements

Andreas Fischer[1], Franck Bertagnolio[1], Wen Zhong Shen[1], Jesper Madsen[2]

[1] Institute for Wind Energy, Technical University of Denmark, Frederiksborgvej 399, DK-4000 Roskilde
[2] LM Wind Power A/S, Jupitervej 6, DK-6000 Kolding

E-mail: asfi@dtu.dk

Abstract. A new CFD RANS based method to predict the far field sound pressure emitted from an aerofoil with serrated trailing edge has been developed. The model was validated by comparison to measurements conducted in the Virginia Tech Stability Wind Tunnel. The model predicted 3 dB lower sound pressure levels, but the tendencies for the different configurations were predicted correctly. Therefore the model can be used to optimise the serration geometry. A disadvantage of the new model is that the computational costs are significantly higher than for the Amiet model for a straight trailing edge. However, it is by decades faster than LES methods.

1. Introduction

Public annoyance due to experienced or perceived noise from wind turbine is a significant barrier for development of wind energy on land. The primary issue is aerodynamic noise. Decreasing the aerodynamic noise will increase the public acceptance of wind energy and accelerate the development of onshore wind energy. Trailing edge serrations have shown to reduce noise from wind turbines significantly [1].

Even though the noise reduction potential of TE serrations for aerofoil sections [2] and wind turbines is experimentally well documented, the mechanisms behind the noise reduction are not fully understood.

Recently, Lyu et al. [3] published an analytical solution for the far field sound emitted from an aerofoil with a serrated trailing edge which showed more promising results than the well known analytical solution by Howe [4]. Using the analytical solution by Lyu et al. [3] we developed a method to predict the noise emitted by an aerofoil with serrated trailing edge based on CFD RANS computations. This method relies also on new advances in computing the convecting surface pressure field as described by Fischer et al. [5].

An experiment in the aero acoustic wind tunnel of Virginia Tech was conducted. The aerodynamic performance and the far field sound pressure emitted from an aerofoil developed for wind turbine blades were measured simultaneously. Two different serration geometries were tested on the aerofoil. The results of this model were compared to the wind tunnel measurements.

2. Wind Tunnel Measurements

2.1. Wind Tunnel Setup

The measurements were conducted in the Virginia Tech Stability Wind Tunnel [6]. It is a closed loop subsonic wind tunnel with a 1.83 m x 1.83 m rectangular removable test section. The length of the test section is 7.3 m. Turbulence intensities of less than 0.05% were reported from measurements in the aerodynamic test section. An acoustic test section with Kevlar walls was used. The acoustic test section is surrounded by anechoic chambers. The Kevlar walls were designed to contain the flow and keep the same aerodynamic performance as with a closed test section while sound waves are transmitted through the walls and can be measured in the anechoic chamber. A microphone array consisting of 117 microphones was located in the starboard anechoic chamber to measure the sound emitted from the aerofoil. The setup is shown in figure 1. The microphone array was located at the position x_1 = -0.627 m, x_2 = -0.124 m

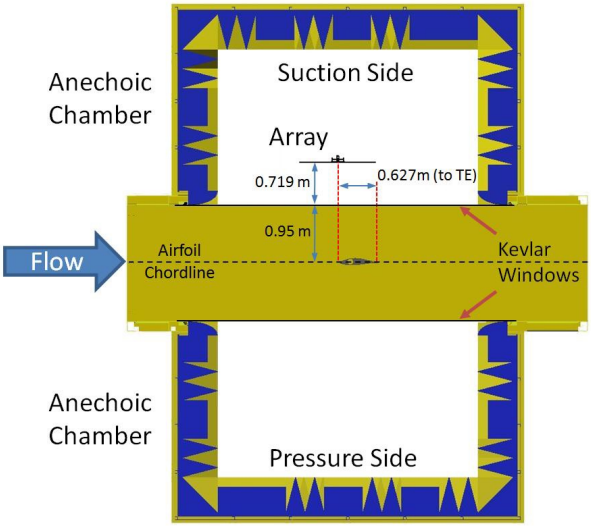

(a) top view

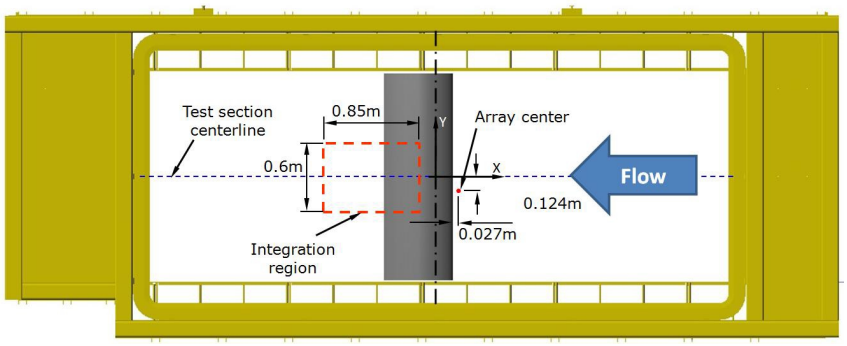

(b) starboard view

Figure 1. The wind tunnel test section, the aerofoil and the microphone array.

and x_3 = 1.669 m in terms of the coordinate system located at the spanwise centre and at the trailing edge of the aerofoil, figure 3. The aerofoil rotated around the quarter chord position and therefore the observer position changed slightly when the angle of attack was changed. For a detailed description of the experiment and data processing the reader is referred to Fischer et al. [7].

2.2. Aerofoil Model and Serrations

The model used in the experiment was a LN118 aerofoil [8]. The aerofoil model had a chord length of 0.6 m and a span of 1.82 m. Two different types of saw-tooth shaped serrations were tested. The serrations are owned by LM Wind Power A/S. The wave length to height ratio of both serrations was $h/\lambda = 1$. The serration with the height 2h = 10 cm were denoted as SER10 and the ones with the height 2h = 15 cm as SER15. The serrations were attached on the pressure side of the aerofoil and bent towards the suction side with a flap angle of 5°.

3. RANS based noise prediction method

The method consists of three steps. First the flow field for a 2D aerofoil configuration is computed with a CFD RANS solver. The boundary layer flow profile and turbulence parameter obtained from this computation are fed into an analytical model to predict the surface pressure. Then the far field sound is computed as function of the convecting surface pressure field.

3.1. CFD RANS Model

The in house code EllipSys2D [9–11] was used to perform the CFD RANS computations. It solves the incompressible RANS equations. The pressure/velocity coupling is realised by using the classical SIMPLE algorithm. Turbulence was modelled with the k-ω Shear Stress Transport (SST) eddy viscosity model [12]. The model for transition was the γ-$\tilde{Re}_\theta$ correlation based model [13]. We ran the code in steady state mode for a 2 dimensional setup. The aerofoil was embedded in a O mesh grid of 40 chord lengths diameter. We used 512 cells on the aerofoil surface and 128 cells in the normal direction. The cell height on the surface was 10^{-6} chord lengths.

The boundary layer flow parameters were computed at x/c = 0.98 on suction and pressure side. The CFD RANS computation provides the mean velocity gradient $\frac{dU}{dz}$ in the boundary layer, the turbulent kinetic energy k_t and the dissipation ϵ. The variance of vertical velocity is calculated via $w^2 = \frac{4}{9}k_t$ (assuming the empirical relation $u^2 : v^2 : w^2 = 1 : \frac{3}{4} : \frac{1}{2}$ by [14]). For the length scale of the von Karman spectrum was calculated by

$$\Lambda = \alpha_\Lambda \frac{k_t^{3/2}}{\epsilon} \tag{1}$$

with the value $\alpha_\Lambda = 0.5188$ as proposed by [15].

3.2. Surface Pressure Model

The analytical solution for the convecting surface pressure field was derived by Kraichnan [16]. He solved the Poisson equation for incompressible boundary layer flow on an infinite plane, figure 2. The cross spectrum of the wall normal velocity has to be modelled in order to close

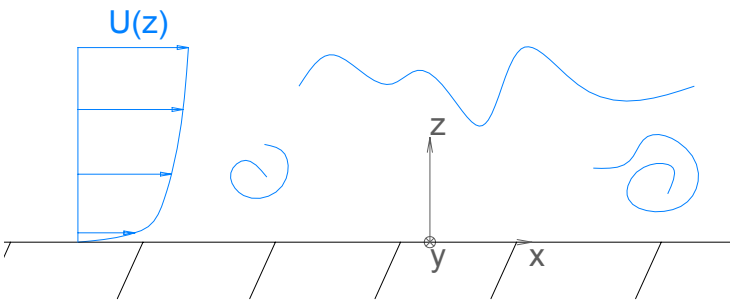

Figure 2. Turbulent boundary layer flow on infinite plane.

the equation. This approach has recently been revised by Fischer et al. [5]. The equation

$$\Pi = 4\rho_0^2 \int_{z=0}^{\infty}\int_{z'=0}^{\infty} (k_1/\kappa)^2 \frac{dU}{dz}(z')\sqrt{w^2(z')} \\ \gamma_{33}(k_1,k_2,z,z')\phi_m(\omega - U_c k_1)e^{-\kappa z'}dz' \frac{dU}{dz}(z)\sqrt{w^2(z))}\phi_{33}(k_1,k_2,y)e^{-\kappa z}dz \tag{2}$$

for the surface pressure frequency wave number spectrum Π was derived. The auto spectrum of the vertical velocity fluctuations ϕ_{33} is given by

$$\phi_{33} = \frac{4}{9\pi}\Lambda^2\beta_1\beta_2\frac{\eta_1^2+\eta_2^2}{\left[1+\eta_1^2+\eta_2^2\right]^{7/3}}. \tag{3}$$

with

$$\eta_1 = \beta_1\Lambda k_1 \tag{4}$$
$$\eta_2 = \beta_2\Lambda k_2 \tag{5}$$
$$\eta_3 = \beta_3\Lambda k_3. \tag{6}$$

It was derived from the classical von Karman spectrum [17] where the anisotropy parameters β_1, β_2 and β_3 as proposed by Panton and Linebarger [18] were introduced. We used the fixed values $\beta_1 = 1$, $\beta_2 = 0.9$ and $\beta_3 = 0.74$. The cross spectral function of the vertical velocity

$$\gamma_{33}(k_1,k_2,z,z') = \frac{9}{4}\frac{1}{2^{4/3}\Gamma(1/3)}\zeta^{7/3}K_{-7/3}(\zeta). \tag{7}$$

was also derived from the von Karman spectrum. $K_\nu(z)$ is the modified Bessel function of second kind and ζ is defined as

$$\zeta = \frac{|z-z'|}{\beta_3\Lambda}\sqrt{1+\eta_1^2+\eta_2^2}. \tag{8}$$

Further, frozen turbulence was assumed and the moving axis spectrum can be described by the delta function

$$\phi_m = \frac{1}{U_c}\delta(\frac{\omega}{U_c} - k_1). \tag{9}$$

The convection velocity was assumed to be equal to the local flow velocity in the boundary layer

$$U_c(z) = U(z). \tag{10}$$

3.3. Far Field Sound Model

Lyu et al. [3] applied Amiet's method [19] for a serrated edge geometry, figure 3. The first step is to solve for pressure scattered at the trailing edge with Schwartzschild's technique. A Fourier expansion in the spanwise direction is introduced. It leads to an inhomogeneous partial differential equation. Lyu et al. [3] solve the inhomogeneous PDE with an iterative process. The far field sound pressure is computed with Curle's equation [19; 20]. Combining the surface pressure presented in the previous section with the far field model yields the far field sound pressure at the observer position X

$$S(X,\omega) = A^2 4\pi L\frac{1}{\lambda^2}4\rho_0^2\sum_{q=-\infty}^{\infty}\int_{z=0}^{\infty}\int_{z'=0}^{\infty}\frac{k_c^2}{k_c^2+k_{2q}^2}\frac{dU}{dz}(z')\sqrt{w^2(z')}\gamma_{33}(k_c,k_{2q},z,z')\frac{1}{U_c}e^{-\kappa z'}dz' \\ \left|\sum_{m=-\infty}^{\infty}\Theta_m^{(0)}(k_c,k_{2q}) + \Theta_m^{(1)}(k_c,k_{2q}) + \Theta_m^{(2)}(k_c,k_{2q})\right|^2 \frac{dU}{dz}(z)\sqrt{w^2(z))}\phi_{33}(k_c,k_{2q},y)e^{-\kappa z}dz \tag{11}$$

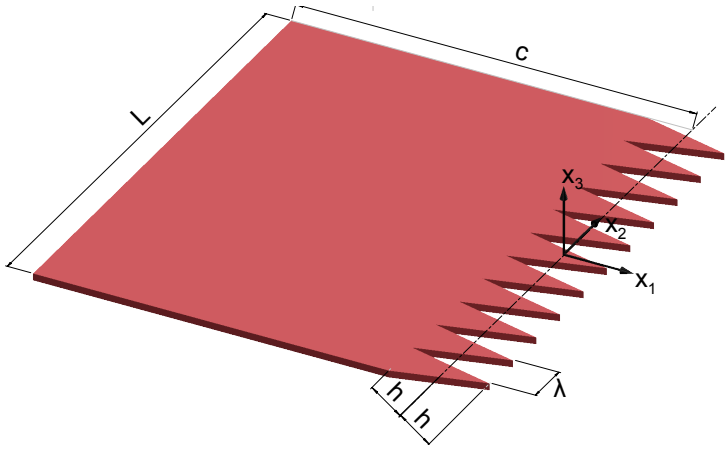

Figure 3. The serration geometry.

where

$$A = \frac{\omega x_3}{4\pi c_0 S_0} \tag{12}$$

is a far field directivity factor,

$$k_c = \frac{\omega}{U_c} \tag{13}$$

is the convective wave number in streamwise direction and

$$k_{2q} = k\frac{x_2}{S_0} + q\frac{2\pi}{\lambda} \tag{14}$$

is the wave number in spanwise direction of Fourier mode q.

$$k = \frac{\omega}{c_0} \tag{15}$$

is the acoustic wave number and c_0 is the speed of sound.
The radiation function of order 0 is defined as

$$\Theta_m^{(0)} = a_m Q_{mm} \tag{16}$$

and the radiation function of order 1 as

$$\Theta_m^{(1)} = \sum_{n=-\infty}^{\infty} v_{mn} a_n \left(ik_c \left[Q_{mm} - Q_{mn} \right] - \sqrt{\mu_n} \left[S_{mm} - S_{mn} \right] \right). \tag{17}$$

For the second order radiation function and the definition of the subfunctions the reader is referred to the paper of Lyu et al. [21]. The solution for the straight trailing edge according to the model of Amiet [19] is

$$\begin{aligned} S(X,\omega) = A^2 4\pi L 4\rho_0^2 \int_{z=0}^{\infty}\int_{z'=0}^{\infty} \frac{k_c^2}{k_c^2+k_2^2}\frac{dU}{dz}(z')\sqrt{w^2(z')}\gamma_{33}(k_c,k_2,z,z')\frac{1}{U_c}e^{-\kappa z'}dz' \\ |\Theta(k_c,k_2)|^2 \frac{dU}{dz}(z)\sqrt{w^2(z))}\phi_{33}(k_c,k_2,z)e^{-\kappa z}dz \end{aligned} \tag{18}$$

where

$$\Theta = \frac{\Gamma}{\nu} \tag{19}$$

is the radiation function. The function

$$\Gamma(c, \mu, \nu) = e^{-i\nu c} E(\mu c) - \sqrt{\frac{\mu}{\mu - \nu}} E((\mu - \nu)c) - \frac{e^{-i\nu c}}{1 - i} \tag{20}$$

was defined by Lyu et al. [3]. The incident pressure is included. c is the chord length of the aerofoil. The derived wave numbers are

$$\mu = \frac{\sqrt{k^2 - \beta^2 k_2^2}}{\beta^2} + k_c + k\frac{M_0}{\beta^2} \tag{21}$$

and

$$\nu = k_c - k\frac{x_1 - M_0 S_0}{\beta^2 S_0}. \tag{22}$$

where $\beta^2 = 1 - M_0^2$. The spanwise wave number is

$$k_2 = k\frac{x_2}{S_0}. \tag{23}$$

If the summation over q, m and n of eq. 11 is truncated at M then the serration model is $(2M + 1)^3$ times more computationally expensive as the model for the straight edge.

4. Results

The far field sound pressure level measured with the microphone array was compared to the sound pressure level predicted by the presented model for the test conditions of a Reynolds number 1.6 million in figure 4. Comparing the measurements for the baseline configuration with

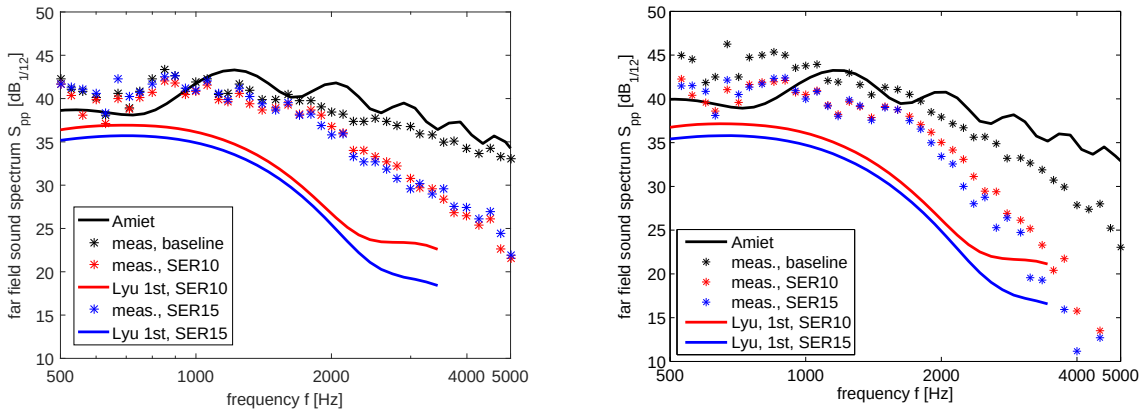

(a) angle of attack -1.3° (b) angle of attack 2.3°

Figure 4. Far field sound pressure level for the LN118 aerofoil at Reynolds number 1.6 million.

Amiet's model we find a difference in slope and level, especially for the high angle of attack, $\alpha = 2.3°$. The model was recently validated extensively in the BANC IV workshop [22] and showed much better agreement with measurements. The reason for the difference could be the array centre location above the leading edge of the aerofoil. The validation test cases were all

measured directly above the trailing edge. The directivity model might not be correct and needs to be investigated further.
The first order solution of the serration model was used. The sum over q, m and n was truncated at $M = 50$ for the lower frequencies. It was necessary to increase M gradually to 80 for the high frequencies. The model got computationally more expensive with increasing frequency. The first order serration model underestimated the measurements by about 3 dB, but the tendency between the different serration geometries was predicted correctly. I.e. the model predicted that SER10 is louder than SER15 which was confirmed by the measurements. Furthermore, the relative difference between the baseline computation and the computation for serrations was in good agreement with the difference between the baseline measurements compared to the measurements with serrated trailing edge.
The baseline model predicted a wavy pattern of the sound pressure level as function of the frequency. The serration model doesn't predict such a wavy pattern. This was probably because of the interference of the coupled modes at the serrated trailing edge. The measurements were too scattered to confirm or contradict this pattern.
Comparing the pressure and suction side contribution to the far field sound as predicted by the model for the angle of attack of 2.3° (figure 5) the baseline configuration was dominated by the suction side contribution in the low frequency range and by the pressure side contribution in the high frequency range. In the high frequency range the model overpredicted the measurements

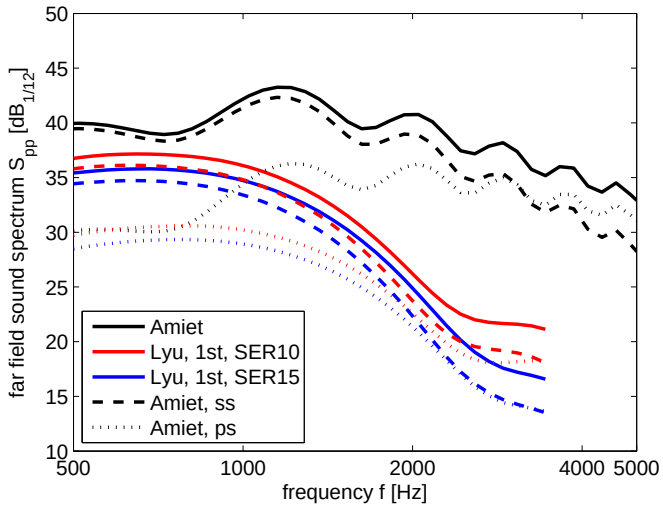

Figure 5. Suction and pressure side contribution to the far field sound pressure level for the LN118 aerofoil at Reynolds number 1.6 million and angle of attack 2.3°.

significantly. Hence, the difference could be attributed to the pressure side calculation. The far field sound computation for the serrated trailing edge was dominated by the suction side contribution. The level had decreased to an insignificant value in the high frequency where the pressure side normally dominates. Therefore the pressure side contribution did not introduce errors in the computations for the serrated geometries.

5. Discussion

A new RANS based method to predict the noise emitted from an aerofoil with serrated trailing edge was developed based on the method to compute the surface pressure developed by Fischer et al. [5] and the model for the far field sound pressure emitted by serrated trailing edges

developed by Lyu et al. [3]. The model was compared to noise measurements conducted in the Virginia Tech Stability Wind Tunnel for the DTU-CQU LN 118 aerofoil. The computed sound pressure levels were about 3 dB below the measured ones. However, the model predicted correctly the difference between the tested configurations. It can be used for optimisation of the serration geometry.
A disadvantage of the serration model was the high computational costs. The solution procedure involves a spanwise Fourier decomposition of the modes. Summing up the modes increases the computational costs significantly, especially in the high frequency range. The model for the straight trailing edge runs on one CPU in less than one second if the CFD RANS computation is already provided. The model for the serrated trailing edge runs for several hours. The computational costs should be reduced to make the model applicable to optimisation frame works and full rotor computations. However, the RANS based model is still by decades faster than LES methods which are usually used to solve these kind of problems.
The results are very promising and it is planned to further validate the model. The next step is to implement the second order solution. We will try to simplify the model in order to reduce computational costs and integrate it in the rotor noise frame work at DTU Wind Energy.

Acknowledgements
The wind tunnel test was founded by the Energy Technology Development and Demonstration Program (EUDP-2011-I, J. nr. 64011-0094) under the Danish Energy Agency. Parts of the presented work were carried out in the project WINDTRUST: 'Demonstration of more reliable innovative designs on a 2MW Wind turbine' under grant agreement no. 322449 of EU's Seventh Framework Programme for Research (FP7). The authors want to acknowledge Patricio Ravetta from AVEC, Inc. for performing the microphone array measurements and providing the post processed data.

References

[1] Oerlemans S, Fisher M, Maeder T and Kögler K 2009 *AIAA Journal* **47** 1470–1481
[2] Fink M R and Bailey D A 1980 Model Tests of Airframe Noise Reduction Concepts *Proceedings* AIAA Paper 80-0979
[3] Lyu B, Azarpeyvand M and Sinayoko S 2016 *J. of Fluid Mech.* **793** 556–588
[4] Howe M S 1991 *J. Acoust Soc. Am.* **90** 482–487
[5] Fischer A, Bertagnolio F and Madsen H A 2016 Improvement of tno type trailing edge noise models *Proceedings of the ISROMAC 2016* (Honolulu, Hawaii)
[6] Devenport W J, Burdisso R A, Borgoltz A, Ravetta P, Barone M F, Brown K A and Morton M A 2013 *J. Sound Vib.* **332** 3971–3991
[7] Fischer A, Bertagnolio F, Shen W Z, Madsen J, Madsen H A, Bak C, Devenport W and Intaratep N 2014 Wind tunnel test of trailing edge serrations for the reduction of wind turbine noise *Proceedings of Inter-noise 2014* (Melbourne, Australia)
[8] Cheng J, Zhu W J, Fischer A, Garcia N R, Madsen J, Chen J and Shen W Z 2013 *Wind Energ.* DOI:10.1002/we
[9] Sørensen N N 1995 General Purpose Flow Solver Applied to Flow over Hills Risø-R-827-(EN) Risø National Laboratory, Roskilde, Denmark
[10] Michelsen J A 1992 Basis3D - A Platform for Development of Multiblock PDE Solvers Tech. Rep. AFM 92-05 Technical University of Denmark
[11] Michelsen J A 1994 Block Structured Multigrid Solution of 2D and 3D Elliptic PDE's Tech. Rep. AFM 94-06 Technical University of Denmark

[12] Menter F R 1993 Zonal Two-Equations $k-\omega$ Turbulence Models for Aerodynamic Flows *Proceedings* AIAA Paper 93-2906

[13] Menter F R, Langtry R B, Likki S R, Suzen Y B, Huang P G and Völker S 2004 A Correlation-Based Transition Model Using Local Variables, Part I - Model Formulation *Proceedings of ASME Turbo Expo 2004, Power for Land, Sea, and Air* GT2004-53452 (Vienna, Austria)

[14] Wilcox D C 1998 *Turbulence Modeling for CFD, Vol. II* (DCW industries)

[15] Lutz T, Herrig A, Würz W, Kamruzzaman M and Krämer E 2007 *AIAA Journal* **45** 779–785

[16] Kraichnan R 1956 *J. Acoust. Soc. Am.* **28** 378–390

[17] v Karman T 1948 *Proc. Nat. Akad. Sci.* **34** 530–539

[18] Panton R and Linebarger J 1974 *J. Fluid Mech.* **65** 261–287

[19] Amiet R K 1976 *J. Sound Vib.* **47** 387–393

[20] Curle N 1955 *Proceedings of the royal society A: Mathematical, physical and engineering sciences* **231** 1011–1023

[21] Lyu B, Azarpeyvand M and Sinayoko S 2015 A trailing-edge noise model for serrated edges *Proc. of the* 21^{st} *AIAA/CEAS Aeroacoustics Conf.* AIAA Paper 2015-2362 (Dallas, TX, USA)

[22] Herr M, Kamruzzaman M and Bahr C 2016 Fourth workshop on benchmark problems for airframe noise computations (banc-iv) *Proc. of the* 22^{st} *AIAA/CEAS Aeroacoustics Conf.* (Lyon, France)